1985-04

Nimbus-7 CZCS: confirmation of its radiometric sensitivity decay rate through 1982

Mueller, James L.

http://hdl.handle.net/10945/44129

Nimbus-7 CZCS: confirmation of its radiometric sensitivity decay rate through 1982

James L. Mueller

The rates of decay in radiometric sensitivities of channels 1, 2, and 3 of the Nimbus-7 Coastal Zone Color Scanner (CZCS) have been determined using data from the clear water masses of the NE Pacific central gyre. Gain correction coefficients $g(\lambda,N)$ are presented as linear functions of Nimbus-7 orbit number N, which are valid through 1982. Internal consistency in the present analysis and comparison with previously published results suggest that corrected radiances are precise within ~5%.

I. Introduction

The magnitudes and rates of decay in radiometric sensitivities of the Nimbus-7 Coastal Zone Color Scanner (CZCS) channels 1, 2, and 3 were recently estimated by Gordon *et al.*,[1] who assumed that CZCS channel 4 (670 nm) had not experienced significant degradation. The purpose of the present paper is to report an independent determination of the time-dependent decay in radiometric sensitivities of CZCS channels 1, 2, and 3. The present results generally confirm the decay models of Gordon *et al.*,[1] but a linear decay model is proposed here for channel 1, in preference to their quadratic form.

The present radiometric decay correction model is fit to CZCS data spanning Nimbus-7 orbits 4944 (late 1979) through 20489 (late 1982). Estimates of calibration adjustment factors were derived by comparing CZCS data with modeled estimates of $L_w(\lambda)$, the upwelled radiance just above the sea surface, for pixels in the central water masses of the subtropical anticyclonic gyre in the NE Pacific Ocean. *In situ* observations of the irradiance attenuation coefficient $K(490)$ throughout this region fall within ~15% of 0.0340 m^{-1}. By assuming random values of $K(490)$ within this narrow range, it is possible to calculate estimates of $L_w(443)$ with sufficient certainty to usefully estimate the magnitude of sensitivity loss in CZCS channel 1.

II. Method of Analysis

The analysis of CZCS radiometric performance is developed from the atmospheric correction algorithm as discussed in detail by Gordon *et al.*,[2] the "clear water radiance" model developed by Gordon and Clark[3] for $\lambda = 520$ and 550 nm, and the $K(490)$ algorithm of Austin and Petzold.[4] The total radiance measured by the CZCS at a clear-water pixel may be expressed as

$$g(\lambda,N)L_t(\lambda) = L_r(\lambda) + t_d(\lambda)L_w(\lambda) + S(\lambda,670) \times [L_t(670) - L_r(670) - t_d(670)L_w(670)], \quad (1)$$

where $L_t(\lambda) = A(\lambda)DN(\lambda) + B(\lambda)$ is calibrated radiance in mW cm^{-2} sr^{-1} μm^{-1} at wavelength λ obtained from the CZCS digital counts $DN(\lambda)$ using the prelaunch calibration coefficients $A(\lambda)$ and $B(\lambda)$ given in Table IV of Gordon *et al.*,[2] and

$$g(\lambda,N) = \frac{C(\lambda)}{f(\lambda,N)} \quad (2)$$

is the adjustment factor required to account for time-dependent loss of radiometric sensitivity in the channel with wavelength λ, and for Nimbus-7 orbit number N. Note that the use of $g(\lambda,N)$ in Eq. (1) combines the two-step calibration adjustment used by Gordon *et al.*[1,2]: their initial adjustment coefficient $C(\lambda)$ (their Table IV), and their time-dependent decay factor $f(\lambda,N)$.

The other terms in Eq. (1) are defined in detail by Gordon *et al.*[2] and will not be discussed here. Values used for extraterrestrial solar irradiance are also taken from Gordon *et al.*[2] (Table IV).

In the exclusively clear-water pixels selected for analysis here, it is safe to assume $L_w(670) = 0$, which is the standard form of the atmospheric correction algorithm presented in Gordon *et al.*[2] It is also assumed that scene-to-scene variability in the aerosol wavelength dependence factor $S(\lambda,N)$ may be parametrized as $(\lambda/670)^n$, where the aerosol Angstrom exponent n is assumed constant in a particular scene.

Using equations given by Gordon and Clark,[3] upwelled radiances $L_w(520)$ and $L_w(550)$ may be modeled

---

The author is with Naval Postgraduate School, Oceanography Department, Monterey, California 93943.

Received 22 October 1984.

Table I. Selected CZCS Data from the NE Pacific Central Gyre

Case	Day	Year	Nimbus-7 orbit	Gain	CZCS digital counts (0...255)			
					$\lambda = 443$	520	550	670 nm
1	289	1979	4944	2	158	124	119	102
2	289	1979	4944	2	144	112	108	90
3	273	1979	4723	2	154	118	112	88
4	312	1979	5262	3	155	124	121	106
5	312	1979	5262	3	156	130	129	124
6	327	1979	5469	2	131	106	102	87
7	327	1979	5469	2	109	88	85	70
8	138	1980	7901	1	150	126	123	105
9	138	1980	7901	1	147	125	121	107
10	193	1980	8661	1	144	126	122	104
11	245	1982	19480	1	124	111	114	115
12	245	1982	19480	1	116	104	105	98
13	278	1982	19936	1	100	92	94	90
14	278	1982	19936	1	105	96	97	94
15	289	1982	20088	1	91	85	86	83
16	307	1982	20337	2	125	120	126	128
17	307	1982	20337	2	106	102	106	110
18	318	1982	20489	2	111	106	112	121
19	318	1982	20489	2	118	116	122	128

for clear-water pixels (phytoplankton pigment concentrations <0.25 mg m^{-3}) with a relative error of ~6%. $L_w(443)$, however, is extremely sensitive to minute variations in phytoplankton pigment concentrations at the low levels characteristic of clear-water pixels. Therefore, it is ordinarily impractical to model $L_w(443)$ with useful accuracy. In this study this difficulty is circumvented by choosing clear-water pixels from a broad oceanic regime which has been observed to be both exceptionally clear and horizontally homogeneous in its vertically integrated optical properties. (This is conceptually similar to the selection of pixels by Gordon *et al.*[2] from regions where historical observations indicate exceptionally low pigment concentrations.)

During the Optical Dynamics Experiment (ODEX) in October and November 1982, vertical profiles of spectral irradiance were measured aboard the R/V Acania at stations along transects extending from the California coast to 143°W near 34°N and from 30°N to 34°N near 142°W. Preliminary calculations of $K(488)$ for ODEX stations west of 125°W fall within the range $0.0302 < K(488) < 0.0398$ m^{-1}. During the same period, R. W. Austin (Scripps Visibility Lab.; personal communication) measured irradiance profiles aboard the R/V DeSteiguer at stations along transects extending from San Diego, Calif., to (30°N, 142°W) and from there to (38°N, 145°W). Values of $K(495)$ for Austin's DeSteiguer stations 2–9, which were all west of 125°W, averaged to 0.0340 m^{-1} with a standard deviation of 0.0024 m^{-1}.

On the basis of the above ODEX and DeSteiguer observations of $K(\lambda)$ at wavelengths near 490 nm, the assumption is made that throughout the geographic region bounded by 28°N to 38°N latitude and by 125°W to 143°W longitude, the irradiance attenuation coefficient $K(490)$ is randomly distributed with mean

$$\overline{K(490)} = 0.034\ \mathrm{m}^{-1} \tag{3}$$

and standard deviation

$$s_K = 0.0024\ \mathrm{m}^{-1}.$$

A sample of CZCS data from 19 pixels within the above region was selected for analysis. The digital counts for CZCS channels 1–4, CZCS gain setting, date, and orbit number associated with each pixel are given in Table I. Table II lists the zenith (relative to the local vertical) and azimuth (clockwise from North) angles of the vectors at each pixel pointing to the spacecraft (θ,ϕ) and sun (θ_0,ϕ_0). Tables I and II contain sufficient data to repeat or extend the present analysis, either under modified assumptions or in combination with additional data.

In selecting this data sample, pixels were retained for analysis only if aerosol radiance $L_a(670) < 0.5$ mW cm^{-2} sr^{-1} μm^{-1}. This limit was set slightly higher than the criterion of $L_a(670) < 0.35$ mW cm^{-2} sr^{-1} μm^{-1} adopted by Gordon *et al.*,[1] because sample size and data distribution over time were otherwise inadequate for analysis.

In addition to the data in Tables I and II, values of the aerosol Angstrom coefficient n and clear-water radiance at 443 nm are needed to calculate $g(\lambda,N)$ using Eq. (1). The aerosol Angstrom coefficient for each jth pixel was arbitrarily assigned a random value:

$$n_j = -0.9 + 0.22X_{1j}, \tag{4}$$

where the coefficients have been selected to randomly vary the Angstrom coefficients over a range consistent with the choice adopted by Gordon *et al.*,[1] and X_{1j} is a normal random deviate distributed as $N(0,1)$, (i.e., a random variable distributed according to a Gaussian probability density function with zero mean and unit variance).

Using assumption (3), an irradiance attenuation coefficient was assigned to each jth pixel according to

$$K_j(490) = 0.0340 + 0.0024X_{2j}\ \mathrm{m}^{-1}, \tag{5}$$

Table II. Geographic Locations of Pixels in Table I, Together with Local Zenith and Azimuth (Clockwise from North) Angles of Vectors Pointing to Nimbus-7 (θ,ϕ) and the Sun (θ_0,ϕ_0)

Case	Latitude deg–min	Longitude deg–min	View direction θ (deg)	ϕ (deg)	Solar direction θ_0 (deg)	ϕ_0 (deg)
1	28–25.15 N	133–17.94 W	40.4	076.4	38.7	163.0
2	33–20.06 N	133–38.40 W	33.8	075.9	43.4	164.6
3	34–16.90 N	137–51.64 W	40.0	074.2	38.9	158.0
4	30–02.39 N	132–54.68 W	09.4	078.6	46.8	173.5
5	30–50.50 N	130–53.28 W	05.1	259.9	47.5	176.2
6	31–23.17 N	132–36.63 W	42.3	074.9	53.0	165.5
7	33–43.69 N	128–13.83 W	16.9	077.2	54.6	171.0
8	35–17.89 N	131–26.95 W	45.4	101.2	21.1	134.3
9	36–31.55 N	131–13.27 W	43.0	103.3	21.8	137.1
10	32–25.08 N	127–49.58 W	42.5	105.6	17.8	121.8
11	32–57.77 N	130–24.59 W	29.0	129.3	27.2	154.4
12	35–57.19 N	128–57.78 W	23.5	158.5	29.4	159.8
13	33–29.00 N	127–09.77 W	21.6	108.7	38.3	165.5
14	33–56.22 N	129–48.73 W	33.1	094.9	39.3	161.6
15	37–44.01 N	129–52.54 W	31.5	087.2	48.0	164.2
16	29–32.04 N	134–39.24 W	42.3	075.5	46.2	164.5
17	33–05.22 N	131–18.22 W	20.0	077.6	49.0	169.8
18	30–05.49 N	130–04.43 W	25.8	077.1	49.0	169.3
19	32–37.95 N	134–50.71 W	43.2	074.4	52.4	164.3

where X_{2j} is a normal random deviate distributed as $N(0,1)$.

Values of $L_w(\lambda)$ for $\lambda = 520$ and 550 nm were assigned to each jth pixel according to

$$\begin{aligned} L_{wj}(520) &= L_{wcj}(520)(1 + 0.06X_{3j}), \\ L_{wj}(550) &= L_{wcj}(550)(1 + 0.06X_{4j}), \end{aligned} \tag{6}$$

where $L_{wcj}(\lambda)$ are clear-water radiance calculated by the method of Gordon and Clark,[3] the relative error coefficient of 0.06 is based on their error analysis, and X_{3j} and X_{4j} are random deviates distributed as $N(0,1)$.

Values of $K_j(490)$ and $L_{wj}(550)$ calculated using Eqs. (5) and (6) were then used to estimate $L_{wj}(443)$ as

$$L_{wj}(443) = L_{wj}(550)\left[\frac{K_j(490) - 0.022}{0.0883}\right]^{-0.6707}. \tag{7}$$

Equation (7) is the inverse of the standard CZCS algorithm for $K(490)$ as given by Austin and Petzold.[4]

Equation (1) was then solved for $g(\lambda,N)$ ($\lambda = 443, 520$, and 550 nm) using approximations (4)–(7) and values from Tables I and II for each of the 19 test pixels.

Because CZCS data were not available for orbits $N < 4650$, Gordon *et al.*[1] decay models were used to fill in the sample through the range $0 < N < 3200$ revolutions. Random noise values, scaled according to their error analysis, were added to each $f(\lambda,N)$ before calculating $g(\lambda,N)$ with Eq. (2). Twelve paired sets of N and $g(\lambda,N)$ ($\lambda = 443,520,550$ nm) were thus generated for this range of orbits and combined with the observations of Tables I and II.

The above procedure yielded a sample of thirty-one paired values of orbit number N and decay coefficient $g(\lambda,N)$ for each of the CZCS channels 1, 2, and 3. A linear trend was then calculated giving $g(\lambda,N)$ as

$$g(\lambda,N) = a(\lambda) + b(\lambda)N, \tag{8}$$

where $a(\lambda)$ and $b(\lambda)$ are simple linear regression coefficients, and N is the Nimbus-7 orbit number (~13.8173 orbits per day from launch on 23 Oct. 1978).

Table III. CZCS Radiometric Sensitivity Decay Coefficients $\overline{a(\lambda)}$ and $\overline{b(\lambda)}$ Derived from 20 Replications with Independent Samples of Random Noise; Also Shown are Standard Deviations $s_a(\lambda)$ and $s_b(\lambda)$ of the Regression Coefficients, and the Mean Standard Deviation $\overline{s_g(\lambda)}$ of $g(\lambda,N)$ About the Regression Line

λ (nm)	$\overline{a(\lambda)}$	$s_a(\lambda)$	$\overline{b(\lambda)} \times 10^5$	$s_b(\lambda) \times 10^5$	$\overline{s_g(\lambda)}$
443	0.9947	0.0084	1.788	0.068	0.040
520	0.9642	0.0024	0.697	0.027	0.020
550	0.9406	0.0041	0.428	0.039	0.020

III. Results

The regression analysis outlined above was replicated with 20 independent samples of random noise to reduce the dependence of the regression coefficients on particular values assumed using Eqs. (4)–(7). The regression coefficients $\overline{a(\lambda)}$ and $\overline{b(\lambda)}$ and residual standard deviations $\overline{s_g(\lambda)}$ of $g(\lambda,N)$ about the regression line are given in Table III as averages over the 20 replications. Also given in Table III are the standard deviations of the regression coefficients, $s_a(\lambda)$ and $s_b(\lambda)$, over the 20 replications.

One example of the scatter in $g_r(\lambda,N)$ about the mean trend [calculated using $\overline{a(\lambda)}$ and $\overline{b(\lambda)}$] is illustrated in Fig. 1. Visual inspection of this, and the scatter plots for the other replications, gives no suggestion that the data would be better fit by a nonlinear model. A significant test for linearity would, however, require several additional observations distributed over the interval between orbits 10,000 and 20,000.

Given coefficients $a_r(\lambda)$ and $b_r(\lambda)$ and values of $L_{wcj}(520)$ and $L_{wcj}(550)$ [as in Eq. (6) but without noise], estimates of n_{jr} and $K_{jr}(490)$ were calculated for each of the $j = 1 \ldots 19$ pixels and $r = 1 \ldots 20$ replications. Similarly, nominal estimates of these variables were calculated for each jth pixel using the mean coefficients $\overline{a(\lambda)}$ and $\overline{b(\lambda)}$ (Table III). The standard deviations of these estimates, s_{nj} and s_{Kj} calculated over the 20 rep-

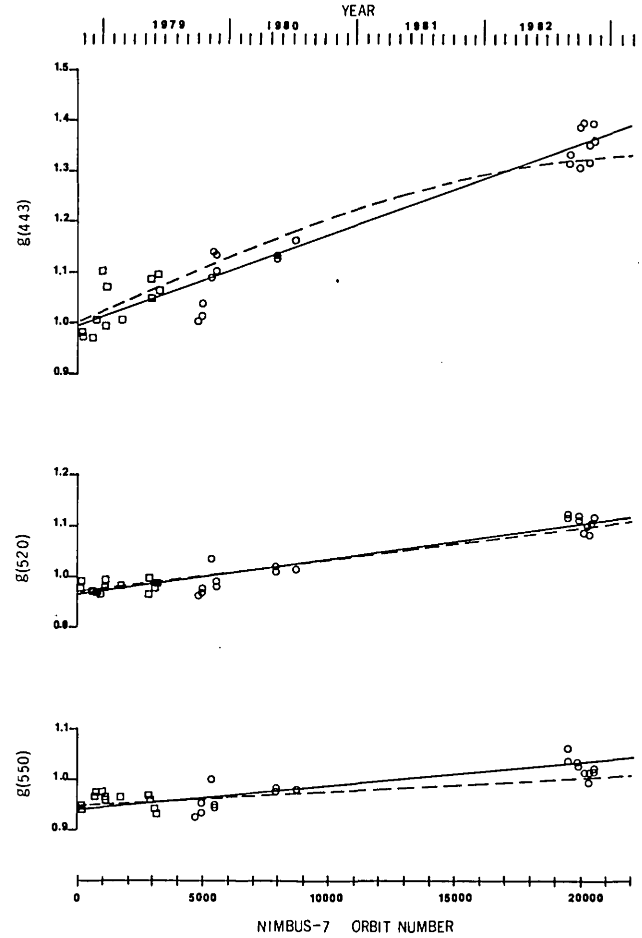

Fig. 1. Corrections for radiometric sensitivity decay of the Nimbus-7 CZCS through its first four years of operation for channels 1, 2, and 3 (443, 520, and 550 nm). The linear regression models (solid lines) are the average fits over 20 replications with independent samples of Gaussian random noise. The circles represent decay coefficients calculated for pixels in the central water masses of the NE Pacific subtropical gyre. Squares are data points generated using the radiometric sensitivity decay correction models of Gordon *et al.*[1] with random noise, and the dashed lines illustrate their models.

lications for each jth pixel, indicate the sensitivity of these derived parameters to uncertainty in regression estimates of $g_r(\lambda,N)$.

The standard deviations of retrieved aerosol Angstrom coefficients (s_{nj}) averaged 0.073, which is ~33% of the random variability assumed in Eq. (4). In all cases analyzed here, this translates to a relative variation of <5% in aerosol wavelength dependence, $(443/670)^n$, due to variations in $a_r(\lambda)$ and $b_r(\lambda)$.

The retrieved values of $K(490)$ at pixel 19 (Table I) averaged to 0.0599 m^{-1}, which is clearly outside the limits assumed in Eq. (3); this case should be excluded in any future analysis of this type.

When pixel 19 is excluded, the average standard deviations in retrieved $K(490)$ are 0.0011 m^{-1} or 46% of the random variation level assumed in Eq. (5). Again, this translates to a relative variation of only 5% in $K(490)$ due to $a_r(\lambda)$ and $b_r(\lambda)$ uncertainty.

IV. Summary and Conclusions

The rates of decay in radiometric sensitivities in CZCS channels 1–3 have been determined from observations of clear-water masses in the central gyre of the NE Pacific Ocean. Recent observations support assumption (3) that $K(490)$ is nearly constant in these water masses. This assumption allows $L_w(443)$, as well as $L_w(520)$ and $L_w(550)$, to be modeled within useful bounds of uncertainty.

In each of 20 replications, values of $K(490)$ and the aerosol Angstrom coefficient n were randomly selected for each pixel from the normally distributed populations described by Eqs. (4) and (5). $L_w(520)$ and $L_w(550)$ were modeled at each pixel using Eq. (6), with normally distributed random noise. In each case, a gain adjustment factor $g(\lambda,N)$ was calculated to bring the CZCS calibrated radiance $L_t(\lambda)$ into agreement with the modeled value. Then, for each replication, the sample of $g(\lambda,N)$ and orbit number N pairs were fit to a linear, least-squares regression model. The average regression coefficients and standard deviations over the 20 replications are given in Table IV for wavelengths $\lambda = 443$, 520, and 550 nm (corresponding to channels 1, 2, and 3, respectively). The standard deviations of the regression coefficients are <10% of the coefficients, and the residual standard deviation of $g(\lambda,N)$ is <4% of the correction in all channels.

When the individual sets of regression coefficients from the 20 separate replications were used to calculate $K(490)$ and n, variability between replications was <5%. And for both parameters, the variability between replications was less than one-half the standard deviations assumed in Eqs. (4) and (5) for determination of the decay trends.

It is encouraging that the retrieved aerosol Angstrom coefficients and $K(490)$ are relatively insensitive to the exact values of parameters assumed in Eqs. (4)–(8); <5% error in these parameters results from uncertainty in the gain adjustment $g(\lambda,N)$ [within the constraint of assumption (3)]. This robustness, the small variability in coefficients $a_r(\lambda)$ and $b_r(\lambda)$ over the 20 replications (Table III), and the close agreement of the present model with that of Gordon *et al.*[1] (Fig. 1) offer good evidence that the radiometric sensitivity decay rate of the CZCS can be accounted for with acceptable accuracy.

Through the end of 1982, the present decay model [Eq. (8) with coefficients from Table III] and that of Gordon *et al.*[1] are virtually interchangeable. In contrast to their quadratic model of decay in channel 1, however, the present results give no indication of nonlinearity (albeit the sample is insufficient to test conclusively for linearity). For data later than early 1983, the Gordon *et al.*[1] model will provide significantly smaller gain adjustments than the present linear model (Fig. 1). This disagreement clearly highlights the dangers of extrapolating either model beyond the range for which it was derived. To extend these models and resolve whether the trend is linear, a procedure such as that presented here should be repeated using additional data distributed over 1983 through 1984.

I thank R. Zaneveld, R. Smith, H. Pak, and R. W. Austin for use of the unpublished $K(490)$ data used to form the very critical assumption (3) above. This research was supported by the Office of Naval Research (Code 4250A) under work request N000148WR24001. The data processing assistance of Melissa Ciandro, of BDM Services Corp., is gratefully acknowledged. I also thank H. Gordon, whose review comments and suggestions led to many improvements in the manuscript.

References

1. H. R. Gordon, J. W. Brown, O. B. Brown, R. H. Evans, and D. K. Clark, "Nimbus 7 CZCS: Reduction of its Radiometric Sensitivity with Time," Appl. Opt. **22**, 3929 (1983).
2. H. R. Gordon, D. K. Clark, J. W. Brown, O. B. Brown, R. H. Evans, and W. W. Broenkow, "Phytoplankton Pigment Concentrations in the Middle Atlantic Bight: Comparison of Ship Determinations and CZCS Estimates," Appl. Opt. **22**, 20 (1983).
3. H. R. Gordon and D. K. Clark, "Clear Water Radiances for Atmospheric Correction of Coastal Zone Color Scanner Imagery," Appl. Opt. **20**, 4175 (1981).
4. R. W. Austin and T. J. Petzold, "The Determination of the Diffuse Attenuation Coefficient of Sea Water Using the Coastal Zone Color Scanner," in *Oceanography from Space*, J. F. R. Gower, Ed. (Plenum, New York, 1981), pp. 239–256.

Meetings Calendar *continued from page 1036*

1985
June

11–14	Image Science & Technology ICO Conf., Helsinki *P. Oittinen, Helsinki U. Technology, Lab. of Graphic Arts Tech., Tekniikantie 3, 02150 Espoo 15, Finland*
12–14	**Workshop on Optical Fabrication & Testing, OSA Tech. Mtg.,** Cherry Hill *OSA Mtgs. Dept, 1816 Jefferson Pl., N.W., Wash., D.C. 20036*
17–19	Int. Conf. on Chemical Kinetics, Gaithersburg *J. Herron, A147 Chem. Bldg., NBS, Wash., D.C. 20234*
18–21	Instabilities & Dynamics of Lasers & Nonlinear Optical Systems Mtg., Rochester *OSA Mtgs. Dept., 1816 Jefferson Pl., N.W., Wash., D.C. 20036*
23–30	Soc. of Women Engineers Ann. Natl. Convention, Minneapolis *G. Hinschberger, P.O. Box 9542, Minneapolis, Minn. 55440*
24–28	7th Int. Conf. on Laser Spectroscopy, Maui *T. Hansch, Physics Dept., Stanford U., Stanford, Calif. 94305*
24–28	Int. Conf. on Fourier & Computerized Infrared Spectroscopy, Ottawa *L. Baignee, Conf. Services Office, Ottawa, Ontario KIA OR6, Canada*
24–29	Fourier & Computerized Infrared Spectroscopy Int. Conf., Ottawa *Natl. Res. Council of Canada, L. Baignee, Conf. Services Off., Ottawa, Ontario, Canada K1A OR6*
24–5 July	Applied Optics Summer course, London *J. Dainty, Optics Sec., Blackett Lab., Imperial Coll., London SW7 2BZ, England*
24–5 July	Applied Materials Technology: Materials Processing for Process-Sensitive Manufacturing course, Edinburgh *Off. of Summer Session, Rm. E19-356, MIT, Cambridge, Mass. 02139*
25–27	11th Int. Symp. on Machine Processing of Remotely Sensed Data, West Lafayette *D. Morrison, Purdue U./LARS, 1291 Cumberland Ave., West Lafayette, Ind. 47906*
26–28	Int. Congr. on Lasers in Medicine & Surgery, Bologna *Medicina Viva, Viale dei Mille, 140, 43100 Parma, Italy*

July

1–4	Int. Conf. on Dynamical Processes in Excited States of Solids, Villeurbanne *W. Yen, U. of Wisconsin, Physics Dept., 1150 University Ave., Madison, Wisc. 53706*
8–11	3rd Conf. on Coherent Laser Radar: Technology & Applications, Malvern *J. Vaughan, Royal Signals & Radar Establishment, Ministry of Defense, St. Andrews Rd., PD316, Great Malvern, Worcestershire, WR14 3PS, U.K.*
8–12	17th Int. Conf. on Phenomena in Ionized Glasses, Budapest *I. Abonyi Roland Eotvos Physical Soc., P.O. Box 240, 1368 Budapest, Hungary*
8–12	Quality Control for Photographic Processing course, Rochester *J. Compton, RIT, P.O. Box 9887, Rochester, N.Y. 14623*
10–13	Hazards of Light Int. Symp., Manchester *U. of Manchester, R. Gregory, School of Medicine, Oxford Rd., Manchester M13 9PT, U.K.*
14–18	27th Rocky Mountain Conf., Denver *F. Lichte, U.S. Geological Survey, Box 25046, MS 928, DFC, Denver, Colo. 80225*
24–30	14th Int. Conf. on Physics of Electronics & Atomic Collisions, Palo Alto *SRI Int., 333 Ravenswood Ave., Menlo Park, Calif. 94025*
24–31	ICPEAC XIV, Stanford *D. Lorents, SRI Int., Chem. Phys. Lab., Menlo Park, Calif. 94025*
25–28	2nd Int. Symp. on The Stability & Preservation of Photographic Images, Ontario *D. Schultze, SPSE, 7003 Kilworth La., Springfield, Va. 22151*
29–2 Aug.	Optical Propagation, Detection, & Communication course, Cambridge *Dir. of Summer Sessions, Rm. E19-356, MIT, Cambridge, Mass. 02139*
31–8 Aug.	17th Int. Congr. of History of Science, Berkeley *Congr. Secretariat, Off. for History of Science & Tech., 470 Stephens Hall, U. Calif., Berkeley, Calif. 94720*

August

4–8	Photoacoustic, Thermal & Related Sciences mtg., Quebec *L. Bertrand, Departement de genie physique, Ecole Polytechnique, Campus de l'Universite de Montreal, P.O. Box 6079, Succursale A, Montreal H3C 3A7, Canada*

continued on page 1063